

Search for diphoton events with large missing transverse energy in 6.3 fb^{-1} of $p\bar{p}$ collisions at $\sqrt{s} = 1.96 \text{ TeV}$

V.M. Abazov,³⁵ B. Abbott,⁷³ M. Abolins,⁶² B.S. Acharya,²⁹ M. Adams,⁴⁸ T. Adams,⁴⁶ G.D. Alexeev,³⁵ G. Alkhazov,³⁹ A. Alton^a,⁶¹ G. Alverson,⁶⁰ G.A. Alves,² L.S. Ancu,³⁴ M. Aoki,⁴⁷ Y. Arnoud,¹⁴ M. Arov,⁵⁷ A. Askew,⁴⁶ B. Åsman,⁴⁰ O. Atramentov,⁶⁵ C. Avila,⁸ J. BackusMayes,⁸⁰ F. Badaud,¹³ L. Bagby,⁴⁷ B. Baldin,⁴⁷ D.V. Bandurin,⁴⁶ S. Banerjee,²⁹ E. Barberis,⁶⁰ P. Baringer,⁵⁵ J. Barreto,² J.F. Bartlett,⁴⁷ U. Bassler,¹⁸ S. Beale,⁶ A. Bean,⁵⁵ M. Begalli,³ M. Begel,⁷¹ C. Belanger-Champagne,⁴⁰ L. Bellantoni,⁴⁷ J.A. Benitez,⁶² S.B. Beri,²⁷ G. Bernardi,¹⁷ R. Bernhard,²² I. Bertram,⁴¹ M. Besançon,¹⁸ R. Beuselinck,⁴² V.A. Bezzubov,³⁸ P.C. Bhat,⁴⁷ V. Bhatnagar,²⁷ G. Blazey,⁴⁹ S. Blessing,⁴⁶ K. Bloom,⁶⁴ A. Boehnlein,⁴⁷ D. Boline,⁷⁰ T.A. Bolton,⁵⁶ E.E. Boos,³⁷ G. Borissoy,⁴¹ T. Bose,⁵⁹ A. Brandt,⁷⁶ O. Brandt,²³ R. Brock,⁶² G. Brooijmans,⁶⁸ A. Bross,⁴⁷ D. Brown,¹⁷ J. Brown,¹⁷ X.B. Bu,⁷ D. Buchholz,⁵⁰ M. Buehler,⁷⁹ V. Buescher,²⁴ V. Bunichev,³⁷ S. Burdin^b,⁴¹ T.H. Burnett,⁸⁰ C.P. Buszello,⁴² B. Calpas,¹⁵ S. Calvet,¹⁶ E. Camacho-Pérez,³² M.A. Carrasco-Lizarraga,³² E. Carrera,⁴⁶ B.C.K. Casey,⁴⁷ H. Castilla-Valdez,³² S. Chakrabarti,⁷⁰ D. Chakraborty,⁴⁹ K.M. Chan,⁵³ A. Chandra,⁷⁸ G. Chen,⁵⁵ S. Chevalier-Théry,¹⁸ D.K. Cho,⁷⁵ S.W. Cho,³¹ S. Choi,³¹ B. Choudhary,²⁸ T. Christoudias,⁴² S. Cihangir,⁴⁷ D. Claes,⁶⁴ J. Clutter,⁵⁵ M.S. Cooke,⁶⁸ M. Cooke,⁴⁷ W.E. Cooper,⁴⁷ M. Corcoran,⁷⁸ F. Couderc,¹⁸ M.-C. Cousinou,¹⁵ A. Croc,¹⁸ D. Cutts,⁷⁵ M. Ćwiok,³⁰ A. Das,⁴⁴ G. Davies,⁴² K. De,⁷⁶ S.J. de Jong,³⁴ E. De La Cruz-Burelo,³² F. Déliot,¹⁸ M. Demarteau,⁴⁷ R. Demina,⁶⁹ D. Denisov,⁴⁷ S.P. Denisov,³⁸ S. Desai,⁴⁷ K. DeVaughan,⁶⁴ H.T. Diehl,⁴⁷ M. Diesburg,⁴⁷ A. Dominguez,⁶⁴ T. Dorland,⁸⁰ A. Dubey,²⁸ L.V. Dudko,³⁷ D. Duggan,⁶⁵ A. Duperrin,¹⁵ S. Dutt,²⁷ A. Dyshkant,⁴⁹ M. Eads,⁶⁴ D. Edmunds,⁶² J. Ellison,⁴⁵ V.D. Elvira,⁴⁷ Y. Enari,¹⁷ S. Eno,⁵⁸ H. Evans,⁵¹ A. Evdokimov,⁷¹ V.N. Evdokimov,³⁸ G. Facini,⁶⁰ A.V. Ferapontov,⁷⁵ T. Ferbel,^{58,69} F. Fiedler,²⁴ F. Filthaut,³⁴ W. Fisher,⁶² H.E. Fisk,⁴⁷ M. Fortner,⁴⁹ H. Fox,⁴¹ S. Fuess,⁴⁷ T. Gadfort,⁷¹ A. Garcia-Bellido,⁶⁹ V. Gavrilov,³⁶ P. Gay,¹³ W. Geist,¹⁹ W. Geng,^{15,62} D. Gerbaudo,⁶⁶ C.E. Gerber,⁴⁸ Y. Gershtein,⁶⁵ G. Ginter,^{47,69} G. Golovanov,³⁵ A. Goussiou,⁸⁰ P.D. Grannis,⁷⁰ S. Greder,¹⁹ H. Greenlee,⁴⁷ Z.D. Greenwood,⁵⁷ E.M. Gregores,⁴ G. Grenier,²⁰ Ph. Gris,¹³ J.-F. Grivaz,¹⁶ A. Grohsjean,¹⁸ S. Grünendahl,⁴⁷ M.W. Grünewald,³⁰ F. Guo,⁷⁰ J. Guo,⁷⁰ G. Gutierrez,⁴⁷ P. Gutierrez,⁷³ A. Haas^c,⁶⁸ S. Hagopian,⁴⁶ J. Haley,⁶⁰ L. Han,⁷ K. Harder,⁴³ A. Harel,⁶⁹ J.M. Hauptman,⁵⁴ J. Hays,⁴² T. Hebbeker,²¹ D. Hedin,⁴⁹ H. Hegab,⁷⁴ A.P. Heinson,⁴⁵ U. Heintz,⁷⁵ C. Hensel,²³ I. Heredia-De La Cruz,³² K. Herner,⁶¹ G. Hesketh,⁶⁰ M.D. Hildreth,⁵³ R. Hirosky,⁷⁹ T. Hoang,⁴⁶ J.D. Hobbs,⁷⁰ B. Hoeneisen,¹² M. Hohlfeld,²⁴ S. Hossain,⁷³ Z. Hubacek,¹⁰ N. Huske,¹⁷ V. Hynek,¹⁰ I. Iashvili,⁶⁷ R. Illingworth,⁴⁷ A.S. Ito,⁴⁷ S. Jabeen,⁷⁵ M. Jaffré,¹⁶ S. Jain,⁶⁷ D. Jamin,¹⁵ R. Jesik,⁴² K. Johns,⁴⁴ M. Johnson,⁴⁷ D. Johnston,⁶⁴ A. Jonckheere,⁴⁷ P. Jonsson,⁴² J. Joshi,²⁷ A. Juste^d,⁴⁷ K. Kaadze,⁵⁶ E. Kajfasz,¹⁵ D. Karmanov,³⁷ P.A. Kasper,⁴⁷ I. Katsanos,⁶⁴ R. Kehoe,⁷⁷ S. Kermiche,¹⁵ N. Khalatyan,⁴⁷ A. Khanov,⁷⁴ A. Kharchilava,⁶⁷ Y.N. Kharzheev,³⁵ D. Khatidze,⁷⁵ M.H. Kirby,⁵⁰ J.M. Kohli,²⁷ A.V. Kozelov,³⁸ J. Kraus,⁶² A. Kumar,⁶⁷ A. Kupco,¹¹ T. Kurča,²⁰ V.A. Kuzmin,³⁷ J. Kvita,⁹ S. Lammers,⁵¹ G. Landsberg,⁷⁵ P. Lebrun,²⁰ H.S. Lee,³¹ S.W. Lee,⁵⁴ W.M. Lee,⁴⁷ J. Lellouch,¹⁷ L. Li,⁴⁵ Q.Z. Li,⁴⁷ S.M. Lietti,⁵ J.K. Lim,³¹ D. Lincoln,⁴⁷ J. Linnemann,⁶² V.V. Lipaev,³⁸ R. Lipton,⁴⁷ Y. Liu,⁷ Z. Liu,⁶ A. Lobodenko,³⁹ M. Lokajicek,¹¹ P. Love,⁴¹ H.J. Lubatti,⁸⁰ R. Luna-Garcia^e,³² A.L. Lyon,⁴⁷ A.K.A. Maciel,² D. Mackin,⁷⁸ R. Madar,¹⁸ R. Magaña-Villalba,³² S. Malik,⁶⁴ V.L. Malyshev,³⁵ Y. Maravin,⁵⁶ J. Martínez-Ortega,³² R. McCarthy,⁷⁰ C.L. McGivern,⁵⁵ M.M. Meijer,³⁴ A. Melnitchouk,⁶³ D. Menezes,⁴⁹ P.G. Mercadante,⁴ M. Merkin,³⁷ A. Meyer,²¹ J. Meyer,²³ N.K. Mondal,²⁹ G.S. Muanza,¹⁵ M. Mulhearn,⁷⁹ E. Nagy,¹⁵ M. Naimuddin,²⁸ M. Narain,⁷⁵ R. Nayyar,²⁸ H.A. Neal,⁶¹ J.P. Negret,⁸ P. Neustroev,³⁹ H. Nilsen,²² S.F. Novaes,⁵ T. Nunnemann,²⁵ G. Obrant,³⁹ D. Onoprienko,⁵⁶ J. Orduna,³² N. Osman,⁴² J. Osta,⁵³ G.J. Otero y Garzón,¹ M. Owen,⁴³ M. Padilla,⁴⁵ M. Pangilinan,⁷⁵ N. Parashar,⁵² V. Parihar,⁷⁵ S.K. Park,³¹ J. Parsons,⁶⁸ R. Partridge^c,⁷⁵ N. Parua,⁵¹ A. Patwa,⁷¹ B. Penning,⁴⁷ M. Perfilov,³⁷ K. Peters,⁴³ Y. Peters,⁴³ G. Petrillo,⁶⁹ P. Pétroff,¹⁶ R. Piegaia,¹ J. Piper,⁶² M.-A. Pleier,⁷¹ P.L.M. Podesta-Lerma^f,³² V.M. Podstavkov,⁴⁷ M.-E. Pol,² P. Polozov,³⁶ A.V. Popov,³⁸ M. Prewitt,⁷⁸ D. Price,⁵¹ S. Protopopescu,⁷¹ J. Qian,⁶¹ A. Quadt,²³ B. Quinn,⁶³ M.S. Rangel,¹⁶ K. Ranjan,²⁸ P.N. Ratoff,⁴¹ I. Razumov,³⁸ P. Renkel,⁷⁷ P. Rich,⁴³ M. Rijssenbeek,⁷⁰ I. Ripp-Baudot,¹⁹ F. Rizatdinova,⁷⁴ M. Rominsky,⁴⁷ C. Royon,¹⁸ P. Rubinov,⁴⁷ R. Ruchti,⁵³ G. Safronov,³⁶ G. Sajot,¹⁴ A. Sánchez-Hernández,³² M.P. Sanders,²⁵ B. Sanghi,⁴⁷ A.S. Santos,⁵ G. Savage,⁴⁷ L. Sawyer,⁵⁷ T. Scanlon,⁴² R.D. Schamberger,⁷⁰ Y. Scheglov,³⁹ H. Schellman,⁵⁰ T. Schliephake,²⁶ S. Schlobohm,⁸⁰ C. Schwanenberger,⁴³ R. Schwienhorst,⁶² J. Sekaric,⁵⁵ H. Severini,⁷³ E. Shabalina,²³ V. Shary,¹⁸ A.A. Shchukin,³⁸ R.K. Shivpuri,²⁸ V. Simak,¹⁰ V. Sirotenko,⁴⁷ P. Skubic,⁷³ P. Slattery,⁶⁹ D. Smirnov,⁵³ K.J. Smith,⁶⁷ G.R. Snow,⁶⁴ J. Snow,⁷² S. Snyder,⁷¹ S. Söldner-Rembold,⁴³ L. Sonnenschein,²¹ A. Sopczak,⁴¹ M. Sosebee,⁷⁶ K. Soustruznik,⁹ B. Spurlock,⁷⁶ J. Stark,¹⁴ V. Stolin,³⁶ D.A. Stoyanova,³⁸ E. Strauss,⁷⁰ M. Strauss,⁷³ D. Strom,⁴⁸ L. Stutte,⁴⁷ P. Svoisky,³⁴ M. Takahashi,⁴³ A. Tanasijczuk,¹

W. Taylor,⁶ M. Titov,¹⁸ V.V. Tokmenin,³⁵ D. Tsybychev,⁷⁰ B. Tuchming,¹⁸ C. Tully,⁶⁶ P.M. Tuts,⁶⁸ L. Uvarov,³⁹ S. Uvarov,³⁹ S. Uzunyan,⁴⁹ R. Van Kooten,⁵¹ W.M. van Leeuwen,³³ N. Varelas,⁴⁸ E.W. Varnes,⁴⁴ I.A. Vasilyev,³⁸ P. Verdier,²⁰ L.S. Vertogradov,³⁵ M. Verzocchi,⁴⁷ M. Vesterinen,⁴³ D. Vilanova,¹⁸ P. Vint,⁴² P. Vokac,¹⁰ H.D. Wahl,⁴⁶ M.H.L.S. Wang,⁶⁹ J. Warchol,⁵³ G. Watts,⁸⁰ M. Wayne,⁵³ M. Weber,^{8, 47} M. Wetstein,⁵⁸ A. White,⁷⁶ D. Wicke,²⁴ M.R.J. Williams,⁴¹ G.W. Wilson,⁵⁵ S.J. Wimpenny,⁴⁵ M. Wobisch,⁵⁷ D.R. Wood,⁶⁰ T.R. Wyatt,⁴³ Y. Xie,⁴⁷ C. Xu,⁶¹ S. Yacoob,⁵⁰ R. Yamada,⁴⁷ W.-C. Yang,⁴³ T. Yasuda,⁴⁷ Y.A. Yatsunenko,³⁵ Z. Ye,⁴⁷ H. Yin,⁷ K. Yip,⁷¹ H.D. Yoo,⁷⁵ S.W. Youn,⁴⁷ J. Yu,⁷⁶ S. Zelitch,⁷⁹ T. Zhao,⁸⁰ B. Zhou,⁶¹ N. Zhou,⁶⁸ J. Zhu,⁶¹ M. Zielinski,⁶⁹ D. Zieminska,⁵¹ and L. Zivkovic⁶⁸

(The D0 Collaboration*)

- ¹Universidad de Buenos Aires, Buenos Aires, Argentina
²LAFEX, Centro Brasileiro de Pesquisas Físicas, Rio de Janeiro, Brazil
³Universidade do Estado do Rio de Janeiro, Rio de Janeiro, Brazil
⁴Universidade Federal do ABC, Santo André, Brazil
⁵Instituto de Física Teórica, Universidade Estadual Paulista, São Paulo, Brazil
⁶Simon Fraser University, Vancouver, British Columbia, and York University, Toronto, Ontario, Canada
⁷University of Science and Technology of China, Hefei, People's Republic of China
⁸Universidad de los Andes, Bogotá, Colombia
⁹Charles University, Faculty of Mathematics and Physics, Center for Particle Physics, Prague, Czech Republic
¹⁰Czech Technical University in Prague, Prague, Czech Republic
¹¹Center for Particle Physics, Institute of Physics, Academy of Sciences of the Czech Republic, Prague, Czech Republic
¹²Universidad San Francisco de Quito, Quito, Ecuador
¹³LPC, Université Blaise Pascal, CNRS/IN2P3, Clermont, France
¹⁴LPSC, Université Joseph Fourier Grenoble 1, CNRS/IN2P3, Institut National Polytechnique de Grenoble, Grenoble, France
¹⁵CPPM, Aix-Marseille Université, CNRS/IN2P3, Marseille, France
¹⁶LAL, Université Paris-Sud, CNRS/IN2P3, Orsay, France
¹⁷LPNHE, Universités Paris VI and VII, CNRS/IN2P3, Paris, France
¹⁸CEA, Irfu, SPP, Saclay, France
¹⁹IPHC, Université de Strasbourg, CNRS/IN2P3, Strasbourg, France
²⁰IPNL, Université Lyon 1, CNRS/IN2P3, Villeurbanne, France and Université de Lyon, Lyon, France
²¹III. Physikalisches Institut A, RWTH Aachen University, Aachen, Germany
²²Physikalisches Institut, Universität Freiburg, Freiburg, Germany
²³II. Physikalisches Institut, Georg-August-Universität Göttingen, Göttingen, Germany
²⁴Institut für Physik, Universität Mainz, Mainz, Germany
²⁵Ludwig-Maximilians-Universität München, München, Germany
²⁶Fachbereich Physik, Bergische Universität Wuppertal, Wuppertal, Germany
²⁷Panjab University, Chandigarh, India
²⁸Delhi University, Delhi, India
²⁹Tata Institute of Fundamental Research, Mumbai, India
³⁰University College Dublin, Dublin, Ireland
³¹Korea Detector Laboratory, Korea University, Seoul, Korea
³²CINVESTAV, Mexico City, Mexico
³³FOM-Institute NIKHEF and University of Amsterdam/NIKHEF, Amsterdam, The Netherlands
³⁴Radboud University Nijmegen/NIKHEF, Nijmegen, The Netherlands
³⁵Joint Institute for Nuclear Research, Dubna, Russia
³⁶Institute for Theoretical and Experimental Physics, Moscow, Russia
³⁷Moscow State University, Moscow, Russia
³⁸Institute for High Energy Physics, Protvino, Russia
³⁹Petersburg Nuclear Physics Institute, St. Petersburg, Russia
⁴⁰Stockholm University, Stockholm and Uppsala University, Uppsala, Sweden
⁴¹Lancaster University, Lancaster LA1 4YB, United Kingdom
⁴²Imperial College London, London SW7 2AZ, United Kingdom
⁴³The University of Manchester, Manchester M13 9PL, United Kingdom
⁴⁴University of Arizona, Tucson, Arizona 85721, USA
⁴⁵University of California Riverside, Riverside, California 92521, USA
⁴⁶Florida State University, Tallahassee, Florida 32306, USA
⁴⁷Fermi National Accelerator Laboratory, Batavia, Illinois 60510, USA
⁴⁸University of Illinois at Chicago, Chicago, Illinois 60607, USA
⁴⁹Northern Illinois University, DeKalb, Illinois 60115, USA
⁵⁰Northwestern University, Evanston, Illinois 60208, USA
⁵¹Indiana University, Bloomington, Indiana 47405, USA
⁵²Purdue University Calumet, Hammond, Indiana 46323, USA

- ⁵³University of Notre Dame, Notre Dame, Indiana 46556, USA
⁵⁴Iowa State University, Ames, Iowa 50011, USA
⁵⁵University of Kansas, Lawrence, Kansas 66045, USA
⁵⁶Kansas State University, Manhattan, Kansas 66506, USA
⁵⁷Louisiana Tech University, Ruston, Louisiana 71272, USA
⁵⁸University of Maryland, College Park, Maryland 20742, USA
⁵⁹Boston University, Boston, Massachusetts 02215, USA
⁶⁰Northeastern University, Boston, Massachusetts 02115, USA
⁶¹University of Michigan, Ann Arbor, Michigan 48109, USA
⁶²Michigan State University, East Lansing, Michigan 48824, USA
⁶³University of Mississippi, University, Mississippi 38677, USA
⁶⁴University of Nebraska, Lincoln, Nebraska 68588, USA
⁶⁵Rutgers University, Piscataway, New Jersey 08855, USA
⁶⁶Princeton University, Princeton, New Jersey 08544, USA
⁶⁷State University of New York, Buffalo, New York 14260, USA
⁶⁸Columbia University, New York, New York 10027, USA
⁶⁹University of Rochester, Rochester, New York 14627, USA
⁷⁰State University of New York, Stony Brook, New York 11794, USA
⁷¹Brookhaven National Laboratory, Upton, New York 11973, USA
⁷²Langston University, Langston, Oklahoma 73050, USA
⁷³University of Oklahoma, Norman, Oklahoma 73019, USA
⁷⁴Oklahoma State University, Stillwater, Oklahoma 74078, USA
⁷⁵Brown University, Providence, Rhode Island 02912, USA
⁷⁶University of Texas, Arlington, Texas 76019, USA
⁷⁷Southern Methodist University, Dallas, Texas 75275, USA
⁷⁸Rice University, Houston, Texas 77005, USA
⁷⁹University of Virginia, Charlottesville, Virginia 22901, USA
⁸⁰University of Washington, Seattle, Washington 98195, USA
(Dated: August 12, 2010)

We report a search for diphoton events with large missing transverse energy produced in $p\bar{p}$ collisions at $\sqrt{s} = 1.96$ TeV. The data were collected with the D0 detector at the Fermilab Tevatron Collider, and correspond to 6.3 fb^{-1} of integrated luminosity. The observed missing transverse energy distribution is well described by the standard model prediction, and 95% C.L. limits are derived on two realizations of theories beyond the standard model. In a gauge mediated supersymmetry breaking scenario, the breaking scale Λ is excluded for $\Lambda < 124$ TeV. In a universal extra dimension model including gravitational decays, the compactification radius R_c is excluded for $R_c^{-1} < 477$ GeV.

PACS numbers: 14.80.Ly, 14.80.Rt, 13.85.Rm

In the standard model (SM), events with two high transverse momentum photons ($\gamma\gamma$) and large missing transverse energy (\cancel{E}_T) are produced at a small rate in $p\bar{p}$ collisions. This final state is therefore sensitive to contributions from processes beyond the SM (BSM). We report a search for $\gamma\gamma$ events with large \cancel{E}_T produced in $p\bar{p}$ collisions recorded using the D0 detector at the Fermilab Tevatron Collider. The sensitivity is assessed for two benchmark BSM models, gauge mediated supersymmetry (SUSY) breaking (GMSB) [1] and universal extra dimensions (UED) [2].

In GMSB models, the masses of the SUSY partners to SM particles arise from SM gauge interactions and are proportional to the effective SUSY breaking scale Λ . As the grav-

itino (\tilde{G}) does not participate in SM gauge interactions, it has a small mass [3] and is the lightest SUSY particle. Assuming R parity conservation [4], the SUSY process with the largest cross section at the Tevatron would be chargino and neutralino pair production ($\chi_1^\pm \chi_2^0, \chi_1^\pm \chi_1^\mp$) [5], followed by decay chains to the next-to-lightest SUSY particle (NLSP). We consider the case when the lightest neutralino (χ_1^0) is the NLSP [6], and decays promptly with the dominant branching fraction yielding a photon and an essentially massless gravitino ($\chi_1^0 \rightarrow \tilde{G}\gamma$) [7]. The two gravitinos escape detection, resulting in the final state $\gamma\gamma + \cancel{E}_T + X$, where X denotes leptons and jets produced in the decay chains [8].

In UED models, extra spatial dimensions are predicted that are accessible to all SM fields. We consider the case of a single UED that is compactified with radius R_c , resulting in a tower of states for each SM field, called Kaluza-Klein (KK) excitations, with the masses of these states separated by R_c^{-1} . At the Tevatron, the UED process with the largest cross section would be the production of pairs of first level KK quarks [9], followed by decay chains to the lightest KK particle (LKP),

*with visitors from ^aAugustana College, Sioux Falls, SD, USA, ^bThe University of Liverpool, Liverpool, UK, ^cSLAC, Menlo Park, CA, USA, ^dICREA/IFAE, Barcelona, Spain, ^eCentro de Investigacion en Computacion - IPN, Mexico City, Mexico, ^fECFM, Universidad Autonoma de Sinaloa, Culiacán, Mexico, and ^gUniversität Bern, Bern, Switzerland.

the KK photon (γ^*). If additional larger extra dimensions also exist that are only accessible to gravity, the LKP is able to decay promptly through gravitational interactions to a photon and a graviton ($\gamma^* \rightarrow G\gamma$) [10, 11]. The two gravitons escape detection, resulting in the final state $\gamma\gamma + \cancel{E}_T + X$.

Searches for BSM physics in $\gamma\gamma + \cancel{E}_T + X$ events have been performed at the CERN e^+e^- Collider (LEP) [12], and at the Tevatron in Run I [13] and Run II [14–17]. This analysis uses similar methods to those adopted in Ref. [17], a six times larger dataset, and improved photon identification criteria utilizing a neural network (NN) discriminant recently employed in other analyses [18]. The larger dataset has substantially increased the search sensitivity, and has allowed an improved formulation of the data-derived SM background prediction. The background prediction, including the assessment of systematic uncertainties, was developed using only the $\cancel{E}_T \leq 50$ GeV region of the $\gamma\gamma$ sample. Once finalized, the events with $\cancel{E}_T > 50$ GeV were included in evaluating the consistency with the SM prediction and the sensitivity to the signal models. In addition to substantially improved limits on the GMSB model, this Letter also presents the first limits on the UED model with gravitational decays.

The D0 detector [19] consists of an inner tracker, a liquid-argon/uranium calorimeter, and a muon spectrometer. The tracking system is comprised of a silicon microstrip tracker (SMT) and a central fiber tracker (CFT), both located within a 2 T superconducting solenoidal magnet. A central calorimeter (CC) covers pseudorapidities $|\eta| < 1.1$, and two endcap calorimeters (EC) extend the coverage to $|\eta| < 4.2$, where $\eta = -\ln|\tan(\theta/2)|$, and θ is the polar angle with respect to the proton beam direction. The electromagnetic (EM) section of the calorimeter is segmented in four longitudinal layers (EM i , $i = 1, 4$) with transverse segmentation $\Delta\eta \times \Delta\phi = 0.1 \times 0.1$ (ϕ is the azimuthal angle), except in EM3 where it is 0.05×0.05 . A central preshower detector (CPS) utilizing several layers of scintillating strips, positioned between the solenoid coil and CC, provides a precise measurement of EM shower position. The trajectory of photon candidates is reconstructed by combining the four EM-layer and CPS measurements [17].

The data analyzed were collected with single EM triggers and correspond to an integrated luminosity of $6.3 \pm 0.4 \text{ fb}^{-1}$ [20]. Events containing identified calorimeter noise patterns which could bias the \cancel{E}_T distribution are removed. Diphoton candidate events are selected by requiring at least two photon candidates with transverse energy $E_T > 25$ GeV identified in the CC. Photon candidates are selected from EM clusters reconstructed within a cone of radius $\mathcal{R} \equiv \sqrt{(\Delta\eta)^2 + (\Delta\phi)^2} = 0.2$ by requiring (i) $\geq 95\%$ of the cluster energy be deposited in the EM layers, (ii) the calorimeter isolation variable $I \equiv [E_{\text{tot}}(0.4) - E_{EM}(0.2)]/E_{EM}(0.2)$ be less than 0.10, where $E_{\text{tot}}(\mathcal{R})$ ($E_{EM}(\mathcal{R})$) is the total (EM) energy in a cone of radius \mathcal{R} , (iii) the shower width in EM3 be consistent with an EM shower, (iv) the scalar sum of the transverse momentum (p_T) of tracks originating from the $p\bar{p}$ collision vertex (PV) in a $0.05 < \mathcal{R} < 0.4$ annulus about the cluster centroid be less than 2 GeV, and (v) the cluster not

be spatially matched to a reconstructed track or a significant density of SMT and CFT hits [17]. Further rejection of jets misidentified as photons is achieved with a requirement on the NN discriminant, trained using a set of track, CPS, and calorimeter based variables [18].

Electrons satisfy the same requirements as photons, with the exception of the track veto (item v). Jets are reconstructed with the iterative midpoint algorithm [21] with cone size $\mathcal{R} = 0.5$. The \cancel{E}_T is determined using calorimeter energy depositions with $|\eta| < 4$. Corrections are applied to \cancel{E}_T to calibrate energy from EM objects and jets, and to account for the p_T of muons. There are on average several $p\bar{p}$ interactions per crossing of the beams. The correct PV is identified in $\approx 98\%$ of signal events for the benchmark models. The photon trajectories must indicate that the candidates originate at the PV. This requirement is to ensure an accurate calculation of transverse energy in background events in which the correct PV is less efficiently identified, to suppress non-collision events, and measured to be $\approx 86\%$ efficient using a $Z(\rightarrow ee, \mu\mu) + \gamma$ data sample. To reduce the number of events with significantly mismeasured \cancel{E}_T , events are rejected if the difference in azimuthal angle ($\Delta\phi$) between the highest E_T jet (if present) and \cancel{E}_T is greater than 2.5 radians, or if $\Delta\phi$ between either photon and \cancel{E}_T is less than 0.2 radians. A total of 7934 $\gamma\gamma$ candidate events satisfy these criteria.

SM background events in the $\gamma\gamma$ sample are categorized as arising from instrumental \cancel{E}_T sources (SM $\gamma\gamma$, γ +jet, multi-jet) and genuine \cancel{E}_T sources ($W\gamma$, W +jet, $W/Z + \gamma\gamma$). All backgrounds are measured using data control samples, with the exception of small contributions from $W/Z + \gamma\gamma$ events, which are estimated using Monte Carlo (MC) simulation.

Instrumental \cancel{E}_T is a result of energy mismeasurement in an otherwise E_T balanced event. Instrumental \cancel{E}_T sources in the $\gamma\gamma$ sample are separated into contributions from SM $\gamma\gamma$ events, and events with at least one photon candidate originating from a misidentified jet (misID-jet), *i.e.*, γ +jet and multi-jet events. The difference in energy resolution for real photons and fakes from misidentified jets results in a difference in the shape of the \cancel{E}_T distribution between the two categories.

The \cancel{E}_T shape in SM $\gamma\gamma$ events is modeled using a dielectron (ee) data sample predominantly composed of $Z \rightarrow ee$ events. The ee sample satisfies the same kinematic requirements as the $\gamma\gamma$ sample, with the exception that the ee invariant mass is restricted to an interval about the Z boson peak to reduce genuine \cancel{E}_T contributions (*e.g.*, W +jet, di-boson, and $t\bar{t}$ events). The \cancel{E}_T distribution in ee events is compared with shapes in $Z \rightarrow ee$ and SM $\gamma\gamma$ MC events generated with PYTHIA [22]. These MC samples, and all others used in this Letter, were processed with full GEANT [23] detector simulation and standard reconstruction algorithms. Kinematic differences between the $Z \rightarrow ee$ and SM $\gamma\gamma$ processes are verified with MC to have a negligible impact on the \cancel{E}_T shape. The $Z \rightarrow ee$ MC accurately models ee data for \cancel{E}_T values below $\cancel{E}_T \approx 35$ GeV. Above this value, a more pronounced tail is observed in ee data. The tail in data reflects both mismeasurements not modeled in MC, and a small residual presence of

genuine \cancel{E}_T events in the ee sample. The average of the data and MC shapes is used to model the \cancel{E}_T in SM $\gamma\gamma$ events for values of $\cancel{E}_T > 35$ GeV, and the data-only and MC-only extremes are used to define a systematic uncertainty on this shape.

The \cancel{E}_T shape in misID-jet events is modeled with a data sample satisfying the same requirements as the $\gamma\gamma$ sample with the exception that at least one of the photon candidates fails the NN requirement. Additionally, photon identification requirements (iii) and (iv) are loosened to reduce the statistical uncertainty on the \cancel{E}_T shape. A systematic uncertainty on the \cancel{E}_T shape in events with misidentified jets is obtained by varying the photon identification criteria.

The instrumental \cancel{E}_T background estimate is normalized such that the number of events with $\cancel{E}_T < 10$ GeV is equal to that in the $\gamma\gamma$ sample. The relative contribution of SM $\gamma\gamma$ and misID-jet background events is determined by a fit to the $\gamma\gamma$ sample \cancel{E}_T distribution for $\cancel{E}_T < 20$ GeV. The fit accounts for the small contribution of SM background with genuine \cancel{E}_T in the fit region, and is verified to be insensitive to signal contributions for benchmark model cross sections relevant to this analysis. The SM $\gamma\gamma$ contribution to the $\gamma\gamma$ sample over the full \cancel{E}_T range is $(41 \pm 17)\%$. A systematic uncertainty accounts for changes in the shape of the predicted instrumental \cancel{E}_T distribution arising from the uncertainty in the determination of the SM $\gamma\gamma$ contribution.

SM background with genuine \cancel{E}_T arises from real SM $\gamma\gamma + \cancel{E}_T + X$ events and from events with an electron misidentified as a photon (misID-ele). The misID-ele contribution is derived using an $e\gamma$ data sample, composed primarily of instrumental \cancel{E}_T sources for $\cancel{E}_T < 20$ GeV and $W(\rightarrow e\nu)\gamma$ and $W(\rightarrow e\nu) + \text{jet}$ events at higher \cancel{E}_T values. The instrumental \cancel{E}_T sources are modeled with the previously introduced ee and misID-jet \cancel{E}_T shapes, respectively. The $Z \rightarrow ee$ normalization is determined by fitting the Z boson peak in the $e\gamma$ invariant mass distribution, and the multi-jet \cancel{E}_T shape is normalized to provide the remaining contribution in the $\cancel{E}_T < 10$ GeV region. The presence of real \cancel{E}_T contributions in the $e\gamma$ sample is seen as an excess of events with high \cancel{E}_T values above the predicted contributions from instrumental sources. This excess is well described by $W\gamma$ and $W + \text{jet}$ events. The expected W boson peak is observed in the transverse mass distribution of $e\gamma$ sample events with $\cancel{E}_T > 30$ GeV. The normalization of the $W + \text{jet}$ contribution is determined from a comparison of the data photon NN shape with MC real and fake photon NN shapes [18] in this \cancel{E}_T region. The remaining contribution is in good agreement with PYTHIA $W\gamma$ production after applying a next-to-leading order (NLO) QCD correction [24] and an additional +15% scaling factor accounting for QED final state radiation (FSR) in inclusive W production. The FSR component [25] is determined with data using the $\Delta\mathcal{R}(e,\gamma)$ distribution. The predicted misID-ele contribution to the $\gamma\gamma$ sample equals the excess of high \cancel{E}_T events in the $e\gamma$ sample, scaled by $f_{e\rightarrow\gamma}/(1 - f_{e\rightarrow\gamma})$, where $f_{e\rightarrow\gamma} = 0.020 \pm 0.005$ denotes the rate at which an electron fakes a photon satisfying the selection criteria, as measured with $Z \rightarrow ee$ data.

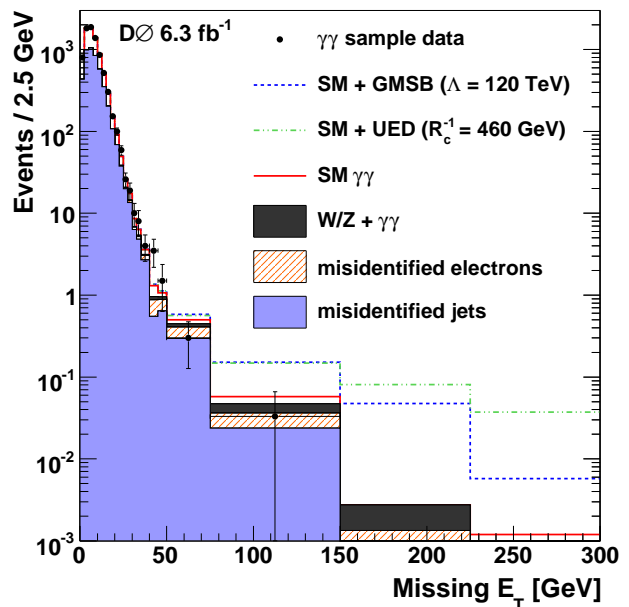


FIG. 1: \cancel{E}_T distribution in the $\gamma\gamma$ sample shown with statistical uncertainty and expected SM background from events with a misidentified jet, a misidentified electron, $W/Z + \gamma\gamma$ events, and SM $\gamma\gamma$ events. The expected \cancel{E}_T distribution in the presence of GMSB and UED events is also displayed for example values of Λ and R_c^{-1} , respectively.

Real SM diphoton events with large genuine \cancel{E}_T originate from $W/Z + \gamma\gamma$ processes. This small background contribution is estimated with MC using MADGRAPH [26]. Events with inclusive W and Z boson decay modes are simulated, with $W \rightarrow l\nu$ ($l = e, \mu, \tau$) and $Z \rightarrow \nu\bar{\nu}$ providing the largest genuine \cancel{E}_T contribution. A total of 1.6 ± 0.1 $W + \gamma\gamma$ events and 3.8 ± 0.3 $Z + \gamma\gamma$ events are estimated to be present in the $\gamma\gamma$ sample. Figure 1 displays the $\gamma\gamma$ sample \cancel{E}_T distribution, which is in good agreement with the SM prediction over the full \cancel{E}_T range. Table I provides the observed number of $\gamma\gamma$ sample events and the SM prediction in three \cancel{E}_T regions.

We determine the sensitivity to the GMSB scenario using a set of values, termed SPS8 [27], for the model parameters. In this set the scale Λ is unconstrained, $M_{mes} = 2\Lambda$, $N_{mes} = 1$, $\tan\beta = 15$, and $\mu > 0$ [27]. The masses and decay widths of SUSY particles are calculated with SUSYHIT 1.3 [28] and used to generate PYTHIA MC events. The event selection efficiency is 0.17 ± 0.02 at $\Lambda = 120$ TeV, and does not differ significantly for other Λ values studied. The NLO production cross section is calculated with PROSPINO 2.1 [5]. The expected \cancel{E}_T distribution for the SM and GMSB at $\Lambda = 120$ TeV is depicted in Figure 1. The number of expected GMSB events in three \cancel{E}_T regions is listed in Table I for $\Lambda = 100$ and 120 TeV.

We consider the UED model as implemented in PYTHIA 6.421 [29], leaving R_c^{-1} unconstrained and setting $\tilde{\Lambda}R_c = 20$, where $\tilde{\Lambda}$ is the cutoff scale for radiative corrections to KK masses. This UED model is implemented in a higher $(4 + N)$ dimensional space, where R_c^{-1} is much larger than

TABLE I: Observed number of $\gamma\gamma$ sample events, predicted background from instrumental \cancel{E}_T sources (SM $\gamma\gamma$, γ +jet, QCD multi-jet) and genuine \cancel{E}_T sources ($W\gamma$, W +jet, $W/Z+\gamma\gamma$), and total predicted SM background, in three \cancel{E}_T intervals. The expected number of GMSB and UED signal events is listed for two Λ and R_c^{-1} values, respectively. The total uncertainty on the SM background and expected signal is given.

\cancel{E}_T Interval, GeV	Observed Events	SM Background Events			Expected Signal Events			
		Instr. \cancel{E}_T	Genuine \cancel{E}_T	Total	GMSB	GMSB	UED	UED
					$\Lambda = 100$ TeV	$\Lambda = 120$ TeV	$R_c^{-1} = 420$ GeV	$R_c^{-1} = 460$ GeV
35 – 50	18	9.6 ± 1.9	2.3 ± 0.5	11.9 ± 2.0	1.8 ± 0.1	0.3 ± 0.1	1.4 ± 0.1	0.3 ± 0.1
50 – 75	3	3.5 ± 0.8	1.5 ± 0.3	5.0 ± 0.9	4.1 ± 0.3	0.8 ± 0.1	2.9 ± 0.2	0.6 ± 0.1
> 75	1	1.1 ± 0.4	0.8 ± 0.1	1.9 ± 0.4	14.3 ± 1.1	4.4 ± 0.4	24.7 ± 2.0	6.4 ± 0.5

that of the N compact extra dimensions accessible to gravity, inducing KK particle decays through gravitational interactions. We choose $N = 6$ and a fundamental Planck scale $M_D = 5$ TeV, such that only the $\gamma^* \rightarrow G\gamma$ decay occurs with appreciable branching fraction [11]. The event selection efficiency is 0.19 ± 0.02 at $R_c^{-1} = 460$ GeV, and does not differ significantly for other R_c^{-1} values studied. The expected \cancel{E}_T distribution for the SM and UED at $R_c^{-1} = 460$ TeV is depicted in Figure 1. The number of expected UED events in three \cancel{E}_T regions is listed in Table I for $R_c^{-1} = 420$ and 460 GeV.

Systematic uncertainties for sources of instrumental \cancel{E}_T are attributed to the uncertainty of the \cancel{E}_T shape in SM $\gamma\gamma$ and misID-jet events, and their relative normalization. An uncertainty in the shape of the \cancel{E}_T distribution for the misID-ele contribution arises from the uncertainty in the $Z \rightarrow ee$ contribution to the $e\gamma$ sample, and a 25% misID-ele normalization uncertainty results from the $f_{e \rightarrow \gamma}$ uncertainty. Systematic uncertainties in the contributions estimated with MC arise from the integrated luminosity (6.1%), trigger efficiency (2%), and photon identification (3% per photon) and trajectories (3%) efficiencies. Uncertainty in parton distribution functions (PDF) [30] yield systematic uncertainties of up to 5% and 20% in the production rate of GMSB and UED events, respectively.

No evidence for BSM physics is observed in the $\gamma\gamma$ sample \cancel{E}_T distribution and limits on the benchmark models are derived using a Poisson log-likelihood ratio test [31] incorporating the full \cancel{E}_T distribution. Pseudo-experiments are generated according to the background-only and signal plus background hypotheses, and account for statistical uncertainty on the expected number of events and systematic uncertainties. The cross section limit is evaluated using the CL_s modified frequentist approach [31]. Figure 2 shows the predicted GMSB and UED cross section with PDF uncertainty, and 95% C.L. cross section exclusion limit, as functions of Λ and R_c^{-1} , respectively. For GMSB, the NLO cross section uncertainty is small compared to the PDF uncertainty. The UED NLO cross section has not yet been computed.

In conclusion, we have presented a search for physics beyond the standard model in the $\gamma\gamma + \cancel{E}_T + X$ final state at the Tevatron. The observed \cancel{E}_T distribution is consistent with the SM expectation and limits on two benchmark models are derived. In the SPS8 GMSB model, values of the effective

SUSY breaking scale $\Lambda < 124$ TeV are excluded at 95% C.L. The limit excludes $m_{\chi_1^0} < 175$ GeV, representing improvements of 50 GeV [17] and 26 GeV [15] with respect to previous measurements. Additionally, the first assessment is made of the sensitivity to the UED model with KK particle decays induced by gravitational interactions, excluding values of the compactification radius $R_c^{-1} < 477$ GeV at 95% C.L.

We thank the staffs at Fermilab and collaborating institutions, and acknowledge support from the DOE and NSF (USA); CEA and CNRS/IN2P3 (France); FASI, Rosatom and RFBR (Russia); CNPq, FAPERJ, FAPESP and FUNDUNESP (Brazil); DAE and DST (India); Colciencias (Colombia); CONACyT (Mexico); KRF and KOSEF (Korea); CONICET and UBACyT (Argentina); FOM (The Netherlands); STFC and the Royal Society (United Kingdom); MSMT and GACR (Czech Republic); CRC Program and NSERC (Canada); BMBF and DFG (Germany); SFI (Ireland); The Swedish Research Council (Sweden); and CAS and CNSF (China).

-
- [1] M. Dine, A.E. Nelson, Phys. Rev. D **48**, 1277 (1993); M. Dine *et al.* Phys. Rev. D **51**, 1362 (1995); M. Dine *et al.*, Phys. Rev. D **53**, 2658 (1996). For a review see G.F. Giudice, R. Rattazzi, Phys. Rept. **322**, 419 (1999).
- [2] T. Appeluqust *et al.*, Phys. Rev. D **64**, 035002 (2001).
- [3] S. Deser, B. Zumino, Phys. Rev. Lett. **38**, 1433 (1977).
- [4] A. Salam, J. Strathdee, Nucl. Phys. B **87**, 85 (1975).
- [5] W. Beenakker *et al.*, Phys. Rev. Lett. **83**, 3780 (1999).
- [6] S.P. Martin, Phys. Rev. D **55**, 3177 (1997).
- [7] P. Fayet, Phys. Lett. B **70**, 461 (1977); Phys. Lett. B **86**, 272 (1979); Phys. Lett. B **175**, 471 (1986).
- [8] S. Dimopoulos *et al.*, Phys. Rev. Lett. **76**, 3494 (1996); S. Ambrosanio *et al.*, Phys. Rev. Lett. **76**, 3498 (1996); K.S. Babu *et al.*, Phys. Rev. Lett. **77**, 3070 (1996); H. Baer *et al.*, Phys. Rev. D **55**, 4463 (1997).
- [9] C. Macesanu *et al.* Phys. Rev. D **66**, 015009 (2002).
- [10] T.G. Rizzo, Phys. Rev. D **64**, 095010 (2001).
- [11] C. Macesanu *et al.* Phys. Lett. B **546**, 253 (2002); C. Macesanu Int. J. Mod. Phys. A **21**, 2259 (2006).
- [12] A. Heister *et al.* (ALEPH Collaboration), Eur. Phys. J. C **28**, 1 (2003); J. Abdallah *et al.* (DELPHI Collaboration) Eur. Phys. J. C **38**, 395 (2005); P. Archard *et al.* (L3 Collaboration), Phys. Lett. B **587**, 16 (2004); G. Abbiendi *et al.* (OPAL Collaboration) Phys. Lett. B **602**, 167 (2004).
- [13] B. Abbott *et al.* (D0 Collaboration), Phys. Rev. Lett. **80**, 442 (1998); F. Abe *et al.* (CDF Collaboration) Phys. Rev. D **59**,

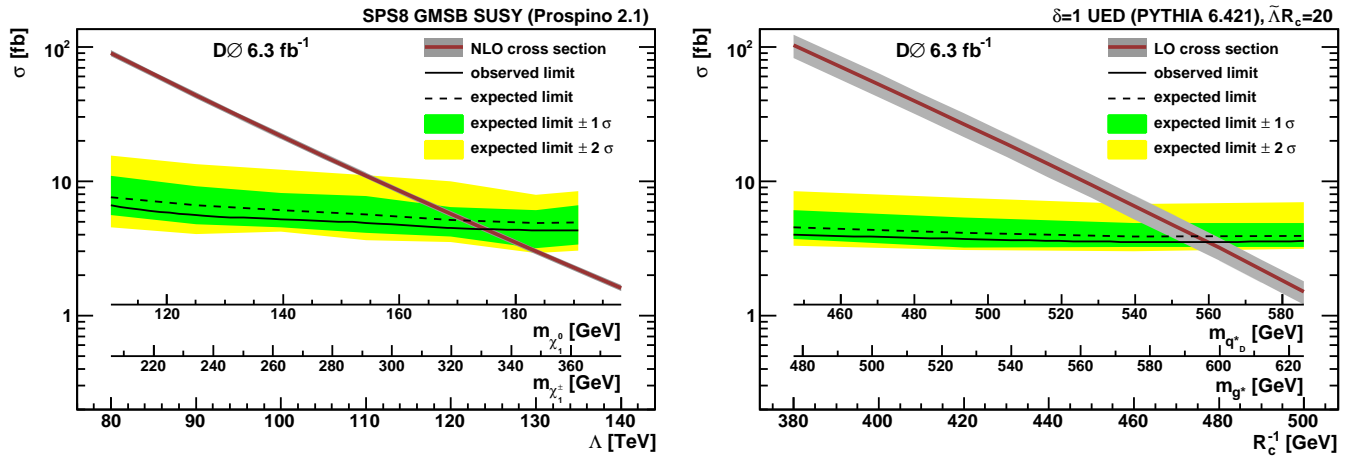


FIG. 2: The predicted cross section for the benchmark GMSB and UED models, and 95% C.L. expected and observed exclusion limits, as a function of Λ and R_c^{-1} , respectively. For the GMSB model, corresponding masses are shown for the lightest chargino, $\chi_{1^\pm}^\pm$, and neutralino, χ_1^0 . For the UED model, corresponding masses are shown for the KK quark, q_D^* , and KK gluon, g^* . The γ^* mass is approximately equal to R_c^{-1} .

- 092002 (1999).
- [14] D. Acosta *et al.* (CDF Collaboration), Phys. Rev. D **71**, 031104 (2005).
- [15] T. Aaltonen *et al.* (CDF Collaboration), Phys. Rev. Lett. **104**, 011801 (2010).
- [16] V.M. Abazov *et al.* (D0 Collaboration), Phys. Rev. Lett. **94**, 041801 (2005).
- [17] V.M. Abazov *et al.* (D0 Collaboration), Phys. Lett. B **659**, 856 (2008).
- [18] V.M. Abazov *et al.* (D0 Collaboration), Phys. Rev. Lett. **102**, 231801 (2009); V.M. Abazov *et al.* (D0 Collaboration), Phys. Lett. B **690**, 108 (2010).
- [19] V.M. Abazov *et al.* (D0 Collaboration), Nucl. Instrum. Methods Phys. Res. A **565**, 463 (2006).
- [20] T. Andeen *et al.*, FERMILAB-TM-2365 (2007).
- [21] G.C. Blazey *et al.*, arXiv:hep-ex/0005012.
- [22] T. Sjöstrand *et al.*, Comput. Phys. Commun. **135**, 238 (2001).
- [23] R. Brun and F. Carminati, CERN Program Library Long Writup W5013, 1993 (unpublished).
- [24] U. Baur *et al.* Phys. Rev. D **48**, 5140 (1993).
- [25] J. Cortes *et al.* Nucl. Phys. B **278**, 26 (1986).
- [26] J. Alwall *et al.*, J. High Energy Phys. **09**, 028 (2007).
- [27] B.C. Allanach *et al.*, Eur. Phys. J. C **25**, 113 (2002).
- [28] A. Djouadi *et al.*, Acta Phys. Polon. B **38**, 635 (2007).
- [29] M. ElKacimi *et al.*, Comput. Phys. Commun. **181**, 122 (2010).
- [30] J. Pumplin *et al.*, J. High Energy Phys. **07**, 012 (2002); D. Stump *et al.*, J. High Energy Phys. **10**, 046 (2003).
- [31] T. Junk, Nucl. Instrum. Methods A **434**, 435 (1999); W. Fisher, FERMILAB-TM-2386-E (2006).